View metadata, citation and similar papers at core.ac.uk

brought to you by CORE

provided by Elsevier - Publisher Connector

Physics Letters B 756 (2016) 147–152

Contents lists available at ScienceDirect

Physics Letters B

www.elsevier.com/locate/physletb

Studying 750 GeV di-photon resonance at photon–photon collider

Hayato Ito *, Takeo Moroi, Yoshitaro Takaesu

Department of Physics, University of Tokyo, Tokyo 113-0033, Japan

ARTICLE INFO

Article history:
Received 15 January 2016
Received in revised form 2 March 2016
Accepted 2 March 2016
Available online 7 March 2016
Editor: J. Hisano

ABSTRACT

Motivated by the recent LHC discovery of the di-photon excess at the invariant mass of ~ 750 GeV, we study the prospect of investigating the scalar resonance at a future photon–photon collider. We show that, if the di-photon excess observed at the LHC is due to a new scalar boson coupled to the standard-model gauge bosons, such a scalar boson can be observed and studied at the photon–photon collider with the center-of-mass energy of ~ 1 TeV in large fraction of parameter space.

© 2016 The Authors. Published by Elsevier B.V. This is an open access article under the CC BY license (http://creativecommons.org/licenses/by/4.0/). Funded by SCOAP[3].

Recently, both ATLAS and CMS Collaborations have reported the results of their analysis of di-photon events. The result of ATLAS, which is based on the 2015 data with the integrated luminosity of 3.2 fb^{-1}, shows the excess with the local (global) significance of 3.6σ (2.0σ) at the di-photon invariant-mass of $M_{\gamma\gamma} \sim 750$ GeV [1]. In addition, the CMS result, which is based on their 2015 data with the integrated luminosity of 2.6 fb^{-1}, also indicates an excess at similar $M_{\gamma\gamma}$; the local significance of the excess is claimed to be 2.6σ (while the global significance is smaller than 1.2σ) [2]. These excesses may indicate the existence of a new resonance Φ with its mass of $m_\Phi \sim 750$ GeV. The production cross section and branching ratio into di-photon are suggested to satisfy [3–8]

$$\sigma(pp \to \Phi \to \gamma\gamma) = \sigma(pp \to \Phi)\mathrm{Br}(\Phi \to \gamma\gamma) \sim 5\text{–}10\ \mathrm{fb}: \text{ at } \sqrt{s_{pp}} = 13\ \mathrm{TeV}, \tag{1}$$

where $\sqrt{s_{pp}}$ is the center-of-mass energy of pp.

One of the explanations of such an excess is a new scalar boson coupled to standard-model gauge bosons via higher dimensional operators [3–100]. The scalar boson may interact as

$$\mathcal{L}_{\mathrm{eff}} = \frac{1}{2\Lambda_i}\varphi\epsilon^{\mu\nu\rho\sigma}\mathcal{F}^{(i),a}_{\mu\nu}\mathcal{F}^{(i),a}_{\rho\sigma}, \tag{2}$$

for the case of pseudo-scalar boson φ, or as

$$\mathcal{L}_{\mathrm{eff}} = \frac{1}{\Lambda_i}\phi\mathcal{F}^{(i),a}_{\mu\nu}\mathcal{F}^{(i),a}_{\mu\nu}, \tag{3}$$

for the case of real scalar boson ϕ. Here, $\mathcal{F}^{(i),a}_{\mu\nu}$ is the field strength of the standard-model gauge bosons where $i = 1$, 2, and 3 correspond to $U(1)_Y$, $SU(2)_L$, and $SU(3)_C$, respectively, and the superscript a denotes the index for the adjoint representations. The summations over the repeated indices are implicit. With these interactions, the scalar boson can be produced at the LHC via the gluon–gluon scattering process, and it can decay into photon pair. Then, the di-photon excess observed at the LHC can be explained by the process of $gg \to \Phi \to \gamma\gamma$ (where $\Phi = \phi$ or φ, and g is gluon).

If there exists such a new scalar boson, the next task for future collider experiments is to precisely study its properties. The LHC will play very important role in such a program [38,101–105]. Here, we consider another possibility, which is the photon–photon collider. The photon–photon collider can be realized at the facility of the International e^+e^- Linear Collider (ILC) by converting electron beam to high energy photons. Because the scalar field of our interest decays into di-photon, it can be produced via the photon–photon scattering process. For the case of the scalar fields with the interactions given in Eq. (2) or (3), one of the advantages of the photon–photon collider is that the single production of the scalar boson is possible so that the kinematical reach is close to the total center-of-mass energy of the collider. In the case of our interest where the mass of the scalar boson is about $m_\Phi \sim 750$ GeV, the scalar boson can be produced at the photon–photon collider with $\sqrt{s_{ee}} \sim 1$ TeV (where $\frac{1}{2}\sqrt{s_{ee}}$ is the energy of the initial-state electron beam), which is within the range of the upgrade ILC. In addition, the clean environment of the photon–photon collider may help precisely studying the properties of the scalar boson.

In this letter, we study the prospect for the study of the scalar boson at the photon–photon collider. Assuming the effective Lagrangian given above, we calculate the production cross section

* Corresponding author.
E-mail address: ito@hep-th.phys.s.u-tokyo.ac.jp (H. Ito).

http://dx.doi.org/10.1016/j.physletb.2016.03.008
0370-2693/© 2016 The Authors. Published by Elsevier B.V. This is an open access article under the CC BY license (http://creativecommons.org/licenses/by/4.0/). Funded by SCOAP[3].

of the scalar boson. Because the effective interaction may originate from the loop effects of heavy vector-like particles or from unknown strong dynamics, we do not specify the origin of the effective Lagrangian and treat Λ_i as free parameters. We also estimate the cross sections for standard-model backgrounds. We will see that, if the di-photon excess observed at the LHC is due to a scalar boson with its mass of $m_\Phi \sim 750$ GeV and couplings given in Eq. (2) or (3), such a new scalar boson can be observed and studied at the photon–photon collider in large fraction of the parameter space. In particular, the cross section for the process $\gamma\gamma \to \Phi \to gg$ is large enough so that such a process can be observed at the photon–photon collider. In addition, some of the processes $\gamma\gamma \to \Phi \to \gamma\gamma$, γZ, ZZ, or W^+W^- may be also observed. With these observations, information about the parameters Λ_i in Eq. (2) or (3) is obtained.

First, we summarize the formulas of the cross sections for the scalar production processes at the LHC and ILC. Hereafter, we concentrate on the case where $\Gamma_\Phi \ll m_\Phi$ (with Γ_Φ being the total decay width of Φ). Then, assuming that the gluon–gluon scattering process is the dominant production process at the LHC, the cross section for the processes $pp \to \Phi \to \gamma\gamma$ is given by

$$\sigma(pp \to \Phi \to \gamma\gamma) = \frac{\pi^2}{8 m_\Phi s_{pp}} \frac{\Gamma(\Phi \to gg)\Gamma(\Phi \to \gamma\gamma)}{\Gamma_\Phi} \times \int dx_1 dx_2 \delta(x_1 x_2 - m_\Phi^2/s_{pp}) g(x_1) g(x_2), \tag{4}$$

where $g(x)$ is the parton distribution function (PDF) of gluon. We use MSTW2008NLO PDF [106], with which the integral in Eq. (4) is evaluated to be 1.7×10^3 for $m_\Phi = 750$ GeV and $\sqrt{s_{pp}} = 13$ TeV. In addition, $\Gamma(\Phi \to gg)$ and $\Gamma(\Phi \to \gamma\gamma)$ are partial decay widths for the gg and $\gamma\gamma$ final states, respectively.

For the monochromatic photon beams, the cross section for the process $\gamma\gamma \to \Phi \to F$ at $\sqrt{s_{\gamma\gamma}} \sim m_\Phi$ (with $\sqrt{s_{\gamma\gamma}}$ being the center-of-mass energy of $\gamma\gamma$) is given by

$$\hat{\sigma}(\gamma\gamma \to \Phi \to F; s_{\gamma\gamma}) = \left(\frac{1 + \xi_2 \xi_2'}{2}\right) \times \frac{16\pi m_\Phi^2}{s_{\gamma\gamma}} \frac{\Gamma(\Phi \to \gamma\gamma)\Gamma(\Phi \to F)}{(s_{\gamma\gamma} - m_\Phi^2)^2 + m_\Phi^2 \Gamma_\Phi^2}, \tag{5}$$

where ξ_2 and ξ_2' are Stokes parameters of the initial-state photons, where $\xi_2 = \pm 1$ corresponds to the photons with helicity ± 1.

At the photon–photon collider, the initial-state photons are provided as back-scattered photons off the electron beams, and are not monochromatic. For the calculation of the cross section at the photon–photon collider, we use the luminosity function of the back-scattered photons given in [107,108]:

$$\frac{1}{L_{ee}} \frac{d^2 L_{\gamma\gamma}}{dy dy'} = f(x, y) B(x, y) f(x, y') B(x, y'), \tag{6}$$

where L_{ee} is the luminosity of the electron beam, y and y' denote the photon energies normalized by the energy of the electron beam $\frac{1}{2}\sqrt{s_{ee}}$, and $x \equiv 2\sqrt{s_{ee}}\omega_0/m_e^2$, with m_e being the electron mass and ω_0 the averaged energy of the laser photons in a laboratory frame. The function f is given in the following form:

$$f(x, y) = \frac{2\pi\alpha^2}{\sigma_c x m_e^2} C_{00}(x, y), \tag{7}$$

where α is the QED fine structure constant, and

$$C_{00}(x, y) = \frac{1}{1 - y} - y + (2r - 1)^2 - \lambda_e P_l x r (2r - 1)(2 - y), \tag{8}$$

with $r \equiv y/x(1 - y)$. In Eq. (8), $\lambda_e/2$ and P_l are the mean helicities of initial electrons and laser photons, respectively. In our numerical calculation, we take $\lambda_e = 0.85$ and $P_l = -1$. In addition,

$$\sigma_c = \sigma_c^{(\mathrm{np})} + \lambda_e P_l \sigma_1, \tag{9}$$

where

$$\sigma_c^{(\mathrm{np})} = \frac{2\pi\alpha^2}{x m_e^2}\left[\left(1 - \frac{4}{x} - \frac{8}{x^2}\right)\ln(x + 1) + \frac{1}{2} + \frac{8}{x} - \frac{1}{2(x + 1)^2}\right], \tag{10}$$

$$\sigma_1 = \frac{2\pi\alpha^2}{x m_e^2}\left[\left(1 + \frac{2}{x}\right)\ln(x + 1) - \frac{5}{2} + \frac{1}{x + 1} - \frac{1}{2(x + 1)^2}\right]. \tag{11}$$

The function B is given by

$$B(x, y) = \begin{cases} \exp\left[-\frac{\rho^2}{8}\left(\frac{x}{y} - x - 1\right)\right] & : \ y_m/2 < y < y_m \\ 0 & : \ \text{otherwise} \end{cases}, \tag{12}$$

where $y_m \equiv x/(x + 1)$, and ρ is the reduced distance between conversion and collision points. We assume the photon–photon collider with $x = 4.8$, which maximizes y_m without spoiling the photon luminosity [107,108], and take $\rho = 1$ in our numerical calculation. In addition, the Stokes parameter is given by

$$\xi_2(y) = \frac{C_{20}(x, y)}{C_{00}(x, y)}, \tag{13}$$

where

$$C_{20}(x, y) = \lambda_e r x\left[1 + (1 - y)(2r - 1)^2\right] - P_l(2r - 1)\left(\frac{1}{1 - y} + 1 - y\right). \tag{14}$$

Notice that $\xi_2(y) \to 1$ as $y \to y_m$. Using the luminosity function of the back-scattered photons, the cross section at the photon–photon collider is given by

$$\sigma(\gamma\gamma \to \Phi \to F) = \frac{1}{L_{ee}} \int_0^{y_m} dy dy' \frac{d^2 L_{\gamma\gamma}}{dy dy'} \hat{\sigma}(\gamma\gamma \to \Phi \to F; s_{\gamma\gamma} = y y' s_{ee}). \tag{15}$$

We normalize the cross section at the photon–photon collider using L_{ee}.

For the calculation of the cross sections, it is important to understand the decay widths of the scalar boson. In the following numerical analysis, we consider the case where the scalar resonance is a pseudo-scalar boson φ. (For $m_\Phi \gg m_Z$, the following results are almost the same even if we consider the case of real scalar boson.) In such a case, adopting the effective Lagrangian given in Eq. (2), the partial decay widths of φ are given by

$$\Gamma(\varphi \to gg) = \frac{2 m_\varphi^3}{\pi \Lambda_3^2}, \tag{16}$$

$$\Gamma(\varphi \to \gamma\gamma) = \frac{m_\varphi^3}{4\pi \Lambda_{\gamma\gamma}^2}, \tag{17}$$

$$\Gamma(\varphi \to \gamma Z) = \frac{m_\varphi^3}{8\pi \Lambda_{\gamma Z}^2}\left(1 - \frac{m_Z^2}{m_\varphi^2}\right)^3, \tag{18}$$

$$\Gamma(\varphi \to ZZ) = \frac{m_\varphi^3}{4\pi \Lambda_{ZZ}^2}\left(1 - \frac{4 m_Z^2}{m_\varphi^2}\right)^{3/2}, \tag{19}$$

$$\Gamma(\varphi \to W^+W^-) = \frac{m_\varphi^3}{2\pi \Lambda_2^2}\left(1 - \frac{4 m_W^2}{m_\varphi^2}\right)^{3/2}, \tag{20}$$

where m_φ, m_Z, and m_W are the masses of pseudo-scalar boson φ, Z boson, and $W^\pm$ boson, respectively, and

$$\Lambda_{\gamma\gamma}^{-1} \equiv \Lambda_2^{-1}\sin^2\theta_W + \Lambda_1^{-1}\cos^2\theta_W, \tag{21}$$

$$\Lambda_{\gamma Z}^{-1} \equiv 2(\Lambda_2^{-1} - \Lambda_1^{-1})\sin\theta_W\cos\theta_W, \tag{22}$$

$$\Lambda_{ZZ}^{-1} \equiv \Lambda_2^{-1}\cos^2\theta_W + \Lambda_1^{-1}\sin^2\theta_W, \tag{23}$$

with θ_W being the Weinberg angle. (The decay widths of the real scalar boson can be found, for example, in [38].) In our analysis, the total decay width is treated as a free parameter, because there may exist decay modes other than $\Phi \to VV'$ (with V and V' denoting standard-model gauge bosons), like the decay into dark matter pairs [10,53,54,63,72,75,109–111]. Thus, there are four free parameters in our analysis, i.e., Λ_1, Λ_2, Λ_3, and Γ_Φ. With $\sigma(pp \to \Phi \to \gamma\gamma)$ being fixed, the cross section $\sigma(\gamma\gamma \to \Phi \to VV')$, which is our primary interest, is insensitive Γ_Φ in particular when $\Gamma_\Phi \ll m_\Phi$, as we discuss in the following.

Using Eq. (15), we calculate the total cross section for the scalar-boson production process at the photon–photon collider. Assuming that the Φ production at the LHC is via the gluon-fusion process, the cross sections $\sigma(\gamma\gamma \to \Phi \to F)$ and $\sigma(pp \to \Phi \to \gamma\gamma)$ are related as

$$\sigma(\gamma\gamma \to \Phi \to F) \simeq \sigma_{gg} \times \frac{\mathrm{Br}(\Phi \to F)}{\mathrm{Br}(\Phi \to gg)} \times \left[\frac{\sigma(pp \to \Phi \to \gamma\gamma; \sqrt{s_{pp}} = 13\ \mathrm{TeV})}{10\ \mathrm{fb}}\right], \tag{24}$$

where σ_{gg} is a numerical constant. (See Eqs. (4), (5) and (15).) In our numerical calculation, we take $\sigma(pp \to \Phi \to \gamma\gamma; \sqrt{s_{pp}} = 13\ \mathrm{TeV}) = 10$ fb. We note here that, although we mostly consider the decay of Φ into gauge-boson pairs, the above equation is applicable to any final state.

We calculate σ_{gg} for the narrow width case (i.e., $\Gamma_\Phi \ll m_\Phi$) as well as for the cases of $\Gamma_\Phi = 25$ and 50 GeV. For the latter cases, the integration in Eq. (15) is performed in the region of $m_\Phi - 2\Gamma_\Phi \le \sqrt{s_{\gamma\gamma}} \le m_\Phi + 2\Gamma_\Phi$, because the photon luminosity function we adopt is reliable only around $\sqrt{s_{\gamma\gamma}} \sim m_\Phi$; we have checked that the result does not change much even if we perform the integration in the region of $m_\Phi - \Gamma_\Phi \le \sqrt{s_{\gamma\gamma}} \le m_\Phi + \Gamma_\Phi$.

In Fig. 1, we plot σ_{gg} as a function of $\sqrt{s_{ee}}$, taking $m_\Phi = 750$ GeV. We can see that σ_{gg} is maximized when $\sqrt{s_{ee}} \sim 950$ GeV. The maximal value of σ_{gg} depends on the width of the scalar boson, and σ_{gg} can be as large as 110–170 fb for $\Gamma_\Phi \lesssim 50$ GeV. We are using the photon luminosity function which has a peak at $\sqrt{s_{\gamma\gamma}} \simeq 0.79\sqrt{s_{ee}}$. Thus, in the narrow width case, σ_{gg} takes its maximal value of 170 fb for $\sqrt{s_{ee}} \simeq 945$ GeV. With the integrated luminosity of $L_{ee} \sim O(1)$ ab^{-1}, the total number of the events at the photon–photon collider is as large as (or larger than) $O(10^5)$, which may make the detailed study of the scalar boson Φ possible at the photon–photon collider. (We note that we neglect the interference between the scalar-boson-exchange and standard-model diagrams, and hence our results are not reliable for the parameter region where the signal cross sections become comparable to the background ones.)

In order to discuss the collider phenomenology of the scalar boson at the photon–photon collider, we need to understand background processes. Assuming the effective Lagrangian given in Eq. (2) or (3), we consider the signal processes of

$$\gamma\gamma \to \Phi \to VV',$$

where $VV' = \gamma\gamma, \gamma Z, ZZ, W^+W^-$, and gg. For these signal events, there exist standard-model backgrounds. In order to estimate the number of backgrounds for $VV' = \gamma\gamma, \gamma Z, ZZ$, and W^+W^-, we calculate the following quantity in the standard-model:

$$\kappa_{VV'} \equiv \left.\frac{d\sigma^{(\mathrm{SM})}(\gamma\gamma \to VV')}{dm_{VV'}}\right|_{|\cos\theta_{\mathrm{CM}}| < \cos\theta_{\mathrm{cut}},\ m_{VV'} = m_\Phi}, \tag{25}$$

where $m_{VV'}$ is the invariant mass of the final-state gauge boson pair. Some of the final-state gauge bosons are likely to be emitted to the beam direction. Thus, in order to reduce the number of backgrounds, the phase-space integration is limited to the region of $|\cos\theta_{\mathrm{CM}}| < \cos\theta_{\mathrm{cut}}$, where θ_{CM} is the angle between initial-state photon and the final-state gauge boson in the center-of-mass frame. Correspondingly, in the calculation of the signal cross section, the phase-space integration should be performed in the region of $|\cos\theta_{\mathrm{CM}}| < \cos\theta_{\mathrm{cut}}$. Because the final-state particles are emitted spherically in the signal events, the effect of limiting the final-state phase space is taken into account by multiplying the total cross section by $\cos\theta_{\mathrm{cut}}$. We expect to reduce the standard-model backgrounds by using the kinematical variable $m_{VV'}$ (as well as $\cos\theta_{\mathrm{CM}}$), and hence the expected numbers of the background events are estimated as

$$N_{VV'}^{(\mathrm{BG})} = L_{ee}\kappa_{VV'}\Delta m_{VV'}, \tag{26}$$

where $\Delta m_{VV'}$ is the width of the bin for the study of the scalar boson production. In the standard model, the processes $\gamma\gamma \to \gamma\gamma$, γZ, and ZZ happen at the loop level, and their cross sections can be found in [112–114]. On the contrary, the process $\gamma\gamma \to W^+W^-$ occurs at the tree level. The cross section for this process is evaluated with the use of `MadGraph5` [115]. The values of $\kappa_{VV'}$ (with $VV' = \gamma\gamma, \gamma Z, ZZ$, and W^+W^-) are summarized in Table 1.

For the gluon–gluon final state, the dominant background is from the pair-production of light quarks, $\gamma\gamma \to \bar{q}q$, because gluon and light-quark jets are indistinguishable. Thus, we calculate

$$\kappa_{\bar{q}q} \equiv \sum_{q=u,d,s,c} \left.\frac{d\sigma^{(\mathrm{SM})}(\gamma\gamma \to \bar{q}q)}{dm_{\bar{q}q}}\right|_{|\cos\theta_{\mathrm{CM}}| < \cos\theta_{\mathrm{cut}}}, \tag{27}$$

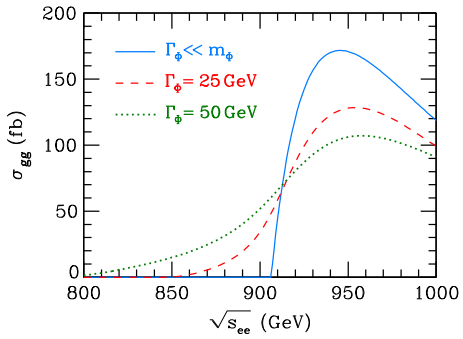

Fig. 1. σ_{gg} as a function of $\sqrt{s_{ee}}$ for $m_\Phi = 750$ GeV. The blue (solid) line is for the narrow width case, while the red (dashed) and green (dotted) ones are for $\Gamma_\Phi =$ 25 and 50 GeV, respectively. (For interpretation of the references to color in this figure legend, the reader is referred to the web version of this article.)

Table 1
The value of $\kappa_{VV'}(\cos\theta_{\mathrm{cut}})$ with $VV' = \gamma\gamma, \gamma Z, ZZ$, and W^+W^- in units of fb/GeV. Here, we take $\sqrt{s_{ee}} = 945$ GeV.

VV'	$\kappa_{VV'}(0.99)$	$\kappa_{VV'}(0.95)$	$\kappa_{VV'}(0.90)$	$\kappa_{VV'}(0.80)$	$\kappa_{VV'}(0.70)$
$\gamma\gamma$	0.057	0.049	0.041	0.032	0.025
γZ	0.36	0.30	0.26	0.20	0.16
ZZ	0.58	0.50	0.42	0.32	0.25
W^+W^-	137	67	42	24	16

Table 2
The value of $\kappa_{\bar{q}q}(\cos\theta_{\rm cut})$ in units of fb/GeV for several values of $m_{\bar{q}q}$. Here, we take $\sqrt{s_{ee}} = 945$ GeV.

$m_{\bar{q}q}$	$\kappa_{\bar{q}q}(0.99)$	$\kappa_{\bar{q}q}(0.95)$	$\kappa_{\bar{q}q}(0.90)$	$\kappa_{\bar{q}q}(0.80)$	$\kappa_{\bar{q}q}(0.70)$
750 GeV	0.44	0.28	0.21	0.14	0.11
725 GeV	1.0	0.62	0.47	0.33	0.24
700 GeV	1.6	1.0	0.75	0.52	0.38

where $m_{\bar{q}q}$ is the invariant mass of the final-state $\bar{q}q$ system, and $\cos\theta_{\rm CM}$ denotes the angle between the initial-state photon and the final-state quark in the center-of-mass frame. (For our numerical calculation, `MadGraph5` is used.) Because we expect a high b-tagging efficiency at the ILC detectors, i.e., $\epsilon_b \sim 70$–80% with the mis-identification efficiency of light quarks being $O(1)\%$ [116], we assume that the $\bar{b}b$ contribution can be largely eliminated and hence is sub-dominant. Thus, we do not include its effect into the calculation of $\kappa_{\bar{q}q}$. We found that $\kappa_{\bar{q}q}$ has a sizable dependence on $m_{\bar{q}q}$, and hence we calculate this quantity for several values of $m_{\bar{q}q}$. The results are shown in Table 2. Importantly, the light-quark pair production cross section is strongly dependent on the polarization of initial-state photons. In particular, the cross section vanishes when the stokes parameters of two initial-state photons satisfy $\xi_2\xi_2' = 1$; with our choice of collider parameters, this relation is realized at the end-point of the spectrum of back-scattered photon, i.e., $y = y' = y_m$. Even at the peak of the photon luminosity function, the product $\xi_2\xi_2'$ is close to 1, and the light-quark pair production cross section is significantly suppressed compared to the case of unpolarized initial-state photons.

Now we discuss the signal-to-background ratio for various final states. For this purpose, we specify relevant size of the bin, $\Delta m_{VV'}$, for the study of the scalar-boson production. If the width of the scalar boson is narrow enough, $\Delta m_{VV'}$ is determined by the detector resolution (where we consider the events with no missing momentum). It is expected that, at the ILC detectors, the energy of charged particles and hadronic jets will be measured with excellent accuracies [116]. With the ILC detectors, the jet energy will be measured with the accuracy of 3% or better for jet energies above 100 GeV. In addition, the energy resolution of the electromagnetic calorimeter of the SiD detector, for example, is expected to be $\delta E/E = 0.17/\sqrt{E} \oplus 1\%$ for electrons or photons, and hence we expect that the energy of the photons emitted by the decay of Φ will be measured with the uncertainty of $\sim 1\%$.

Combining Eq. (24) and Fig. 1, the cross section for the gluon–gluon final state at the photon–photon collider is estimated to be 170 fb in the narrow width case, taking $\sigma(pp \to \Phi \to \gamma\gamma) = 10$ fb and $\sqrt{s_{ee}} = 945$ GeV. (The cross section becomes smaller as Γ_Φ increases.) On the contrary, using the results given in Table 2, the cross section of the $\bar{q}q$ background is significantly smaller than the signal cross section even if we take $\Delta m_{VV'} \sim O(10)$ GeV. Integrating out $\kappa_{\bar{q}q}$ for $0.94\, m_\Phi \le m_{\bar{q}q} \le 1.06\, m_\Phi$, for example, we found that the background cross section is 23 fb for $\cos\theta_{\rm cut} = 0.9$. Thus, it will be possible to observe and study signal events with gluon–gluon final state with the luminosity of $L_{ee} \sim O(0.1\text{–}1)$ fb^{-1} or larger.

For the final states containing weak bosons and photon, with Γ_Φ being fixed, the cross sections depend on Λ_3 through the following ratio:

$$\eta \equiv \frac{\Gamma(\Phi \to \gamma\gamma) + \Gamma(\Phi \to \gamma Z) + \Gamma(\Phi \to ZZ) + \Gamma(\Phi \to W^+W^-)}{\Gamma(\Phi \to gg)}. \tag{28}$$

In the limit of $m_\Phi \gg m_Z$, $\eta \simeq (\frac{1}{8}\Lambda_1^{-2} + \frac{3}{8}\Lambda_2^{-2})\Lambda_3^2$. Then, the cross sections for the processes $\gamma\gamma \to \Phi \to \gamma\gamma$, γZ, ZZ, and W^+W^- depend on two parameters, i.e., η and the ratio Λ_1/Λ_2 (as far as

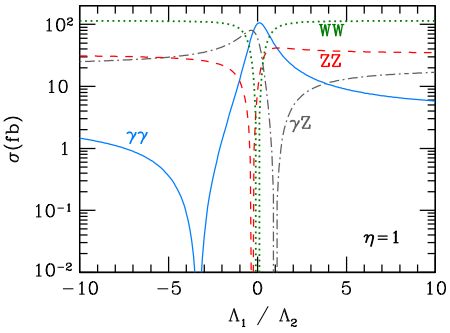

Fig. 2. Cross sections for the processes of $\gamma\gamma \to \Phi \to \gamma\gamma$ (blue solid), γZ (gray dot-dashed), ZZ (red dashed), and W^+W^- (green dotted) as functions of the ratio Λ_1/Λ_2. Here, we take $\sqrt{s_{ee}} = 945$ GeV, $\eta = 1$, and $\sigma(pp \to \Phi \to \gamma\gamma; \sqrt{s_{pp}} = 13\ \text{TeV}) = 10$ fb. (For interpretation of the references to color in this figure legend, the reader is referred to the web version of this article.)

Γ_Φ and $\sigma(pp \to \Phi \to \gamma\gamma)$ are fixed). In addition, the cross sections for these processes are proportional to η for a given value of Λ_1/Λ_2. In Fig. 2, taking $\eta = 1$, we plot the cross sections of these processes as functions of Λ_1/Λ_2. We can see that $\sigma(\gamma\gamma \to \Phi \to \gamma Z)$ becomes suppressed when $\Lambda_1 \simeq \Lambda_2$; this is because, in such a case, the Φ-γ-Z coupling is suppressed (see Eq. (22)). In addition, the cross sections $\sigma(\gamma\gamma \to \Phi \to \gamma\gamma)$ and $\sigma(\gamma\gamma \to \Phi \to ZZ)$ are suppressed when $\Lambda_1 \simeq -\cot^2\theta_W \Lambda_2$ and $\Lambda_1 \simeq -\tan^2\theta_W \Lambda_2$, respectively. We note here that the present scenario is constrained by the searches for the resonances which decay into a pair of electroweak gauge bosons performed at the LHC Run-1. In particular, the negative search for the resonance which decays into γZ final state gives the most stringent constraint. According to [6], for example, the parameter region of $\Gamma(\Phi \to \gamma Z) \gtrsim 2\Gamma(\Phi \to \gamma\gamma)$ is excluded, where we adopted $\sigma(pp \to \Phi \to \gamma\gamma) \sim 10$ fb. The regions of $\Lambda_1/\Lambda_2 \lesssim -1$ and $\Lambda_1/\Lambda_2 \gtrsim 6$ conflict with such a constraint. (If we adopt a smaller value of $\sigma(pp \to \Phi \to \gamma\gamma)$, the constraint becomes weaker.)

Because the cross sections for the processes $\gamma\gamma \to \Phi \to \gamma\gamma$, γZ, ZZ, and W^+W^- are proportional to η with the present parameterization, each mode is expected to be observed at the photon–photon collider if η is large enough. In order to estimate the minimal value of η for the observation of each mode, we calculate the following quantity:

$$S_{VV'}/\sqrt{N_{VV'}^{(\rm BG)}} \equiv \frac{L_{ee}\sigma(\gamma\gamma \to \Phi \to VV')\cos\theta_{\rm cut}}{\sqrt{N_{VV'}^{(\rm BG)}}}. \tag{29}$$

For the processes $\gamma\gamma \to \Phi \to \gamma Z, ZZ$, and W^+W^-, the uncertainties in the measurement of $m_{VV'}$ are expected to be dominated by jet energy resolution, concentrating on the hadronic decay modes of weak bosons. Thus, in the narrow width case, $\frac{1}{2}\Delta m_{VV'}$ is taken to be twice the detector resolution; we adopt $\Delta m_{VV'} = 0.12\, m_\Phi$ for these final states. For $\gamma\gamma \to \Phi \to \gamma\gamma$, we take $\Delta m_{VV'} = 0.04\, m_\Phi$, assuming a good resolution of the electromagnetic calorimeter. Then, we determine the minimal value of η which realizes $S_{VV'}/\sqrt{N_{VV'}^{(\rm BG)}} > 5$. The result is shown in Fig. 3. We note that, if the detector resolution (in particular, for hadronic objects) is not good enough, hadronic decay of $W^\pm$ may be misidentified as that of Z boson. Then, the standard-model W^+W^- production process may also contribute to the background of the signal with ZZ final state with the hadronic decays of Z bosons. Such a problem may be avoided by requiring that at least one of the Z bosons decays into e^+e^- or $\mu^+\mu^-$; if we impose such a requirement, the minimal value of η for $S_{ZZ}/\sqrt{N_{ZZ}^{(\rm BG)}} > 5$ shown in Fig. 3 should be divided by ~ 0.36.

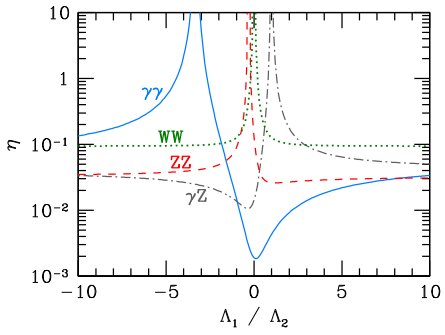

Fig. 3. The minimal values of η to realize $S_{VV'}/\sqrt{N^{(\mathrm{BG})}_{VV'}} > 5$ for $VV' = \gamma\gamma$ (blue solid), γZ (gray dot-dashed), ZZ (red dashed), and W^+W^- (green dotted) as functions of the ratio Λ_1/Λ_2. The size of the bin is taken to be $\Delta m_{VV'} = 0.04 m_\Phi$ (i.e., 30 GeV) for the $\gamma\gamma$ final state, and $\Delta m_{VV'} = 0.12 m_\Phi$ (i.e., 90 GeV) for others. Here, we take $\sqrt{s_{ee}} = 945$ GeV, $\sigma(pp \to \Phi \to \gamma\gamma; \sqrt{s_{pp}} = 13\ \mathrm{TeV}) = 10$ fb, $\cos\theta_{\mathrm{cut}} = 0.9$, and $L_{ee} = 1\ \mathrm{ab}^{-1}$. (For interpretation of the references to color in this figure legend, the reader is referred to the web version of this article.)

We can see that, if $\eta \gtrsim O(10^{-2})$, cross sections for several modes with electroweak gauge boson final states may be measured at the photon–photon collider. With measuring the cross sections of two (or more) of such final states, the ratio Λ_1/Λ_2 can be determined up to two-fold ambiguity. In addition, combined with the information about $\sigma(\gamma\gamma \to \Phi \to gg)$ (or about $\sigma(pp \to \Phi \to \gamma\gamma)$ at the LHC), the quantity η can be determined. (The determination of η may be challenging only with the LHC experiment unless the cross section for the process $pp \to \Phi \to gg$ is measurable at the LHC.) Thus, we will understand the relative size of Λ_i's, from which we will acquire information about the physics behind the higher-dimensional operators given in Eq. (2) or (3). We also note that, if a large amount of the event sample of the process $\sigma(\gamma\gamma \to \Phi \to ZZ)$ is obtained, CP property of Φ may be obtained from the angular correlation of the decay products of Z bosons.

So far, we have assumed that the di-photon events observed at the LHC is due to the scalar-boson production via the gluon–gluon fusion. Another possibility is the production of the scalar boson due to photon–photon collision. In such a case, the cross section for the scalar-boson production at the LHC is estimated as [105]

$$\sigma_{\gamma\gamma}(pp \to \Phi \to \gamma\gamma; \sqrt{s_{pp}} = 13\ \mathrm{TeV}) \simeq 10.8\ \mathrm{pb} \times \left[\frac{\Gamma_\Phi}{45\ \mathrm{GeV}}\right] \mathrm{Br}^2(\Phi \to \gamma\gamma). \tag{30}$$

Then, for the narrow width case, we obtain

$$\sigma(\gamma\gamma \to \Phi \to \gamma\gamma; \sqrt{s_{ee}} = 945\ \mathrm{GeV}) \simeq 4.7\ \mathrm{pb} \times \left[\frac{\sigma_{\gamma\gamma}(pp \to \Phi \to \gamma\gamma; \sqrt{s_{pp}} = 13\ \mathrm{TeV})}{10\ \mathrm{fb}}\right]. \tag{31}$$

(The cross section for other final state F can be obtained by multiplying Eq. (31) by $\mathrm{Br}(\Phi \to F)/\mathrm{Br}(\Phi \to \gamma\gamma)$.) Thus, the cross section for the $\gamma\gamma$ final state is orders of magnitude larger than that of the background (see Table 1), and hence the process $\gamma\gamma \to \Phi \to \gamma\gamma$ will be observed by the photon–photon collider. In addition, the cross sections for the γZ and ZZ final states are typically of the same order of that for the $\gamma\gamma$ final state unless $\Lambda_{\gamma Z}^{-1}$ and Λ_{ZZ}^{-1} are extremely small. The cross section for the W^+W^- final state can be also sizable unless $\Lambda_2 \gg \Lambda_1$. Thus, in this case, detailed studies of the di-photon resonance production with the electroweak gauge boson final states are expected. The detectability of the process of $\gamma\gamma \to \Phi \to gg$ depends on $\mathrm{Br}(\Phi \to gg)$; $S_{gg}/\sqrt{N^{(\mathrm{BG})}_{\bar{q}q}}$ becomes larger than 5 at $L_{ee} = 1\mathrm{ab}^{-1}$ when $\mathrm{Br}(\Phi \to gg)/\mathrm{Br}(\Phi \to \gamma\gamma) \gtrsim 2 \times 10^{-4}$.

Finally, we comment on the production of Φ with the e^+e^- collision. With the interaction given in Eq. (2) or (3), Φ can be produced with the process of $e^+e^- \to \Phi\gamma$ and ΦZ. The Φ production is also possible via the vector-boson fusion processes of $e^+e^- \to \Phi e^+e^-$ and $e^+e^- \to \Phi\bar{\nu}_e\nu_e$. We have estimated the cross section for these processes, taking the center-of-mass energy of 1 TeV. For $\eta = 1$ and $-10 \le \Lambda_1/\Lambda_2 \le 10$, the cross sections for these processes are typically 10^{-1}–10^{-2} fb. Thus, the cross sections at the photon–photon collider are a few orders of magnitude larger. The discussion about the detectability of Φ at the e^+e^- collider requires detailed study of the backgrounds, which we leave for future study.

In summary, we have studied the prospect of investigating a scalar boson Φ at the photon–photon collider, assuming that the recently observed LHC di-photon excess is due to the scalar boson. Assuming also that the scalar-boson production at the LHC is dominated by the gluon–gluon scattering and that $\sigma(pp \to \Phi \to \gamma\gamma) \sim 10$ fb at $\sqrt{s_{pp}} = 13$ TeV, the total cross section for the scalar-boson production at the photon–photon collider with $\sqrt{s_{ee}} \simeq 945$ GeV can be as large as ~ 170 fb (taking $m_\Phi = 750$ GeV). We have also seen that various decay modes of the scalar boson may be observed. Thus, if the existence of the new scalar boson is confirmed with the next run of the LHC, the photon–photon collider can play an important role to study the detailed properties of the scalar boson.

Acknowledgements

The work is supported by Grant-in-Aid for Scientific research Nos. 23104008 and 26400239.

References

[1] ATLAS Collaboration, 2015, ATLAS-CONF-2015-081.
[2] CMS Collaboration, 2015, CMS PAS EXO-15-004.
[3] Y. Nakai, R. Sato, K. Tobioka, arXiv:1512.04924 [hep-ph].
[4] S. Knapen, T. Melia, M. Papucci, K. Zurek, arXiv:1512.04928 [hep-ph].
[5] D. Buttazzo, A. Greljo, D. Marzocca, arXiv:1512.04929 [hep-ph].
[6] R. Franceschini, et al., arXiv:1512.04933 [hep-ph].
[7] S. Di Chiara, L. Marzola, M. Raidal, arXiv:1512.04939 [hep-ph].
[8] J. Ellis, S.A.R. Ellis, J. Quevillon, V. Sanz, T. You, arXiv:1512.05327 [hep-ph].
[9] K. Harigaya, Y. Nomura, arXiv:1512.04850 [hep-ph].
[10] M. Backovic, A. Mariotti, D. Redigolo, arXiv:1512.04917 [hep-ph].
[11] A. Angelescu, A. Djouadi, G. Moreau, arXiv:1512.04921 [hep-ph].
[12] A. Pilaftsis, arXiv:1512.04931 [hep-ph].
[13] T. Higaki, K.S. Jeong, N. Kitajima, F. Takahashi, arXiv:1512.05295 [hep-ph].
[14] S.D. McDermott, P. Meade, H. Ramani, arXiv:1512.05326 [hep-ph].
[15] M. Low, A. Tesi, L.T. Wang, arXiv:1512.05328 [hep-ph].
[16] B. Bellazzini, R. Franceschini, F. Sala, J. Serra, arXiv:1512.05330 [hep-ph].
[17] R.S. Gupta, S. Jäger, Y. Kats, G. Perez, E. Stamou, arXiv:1512.05332 [hep-ph].
[18] C. Petersson, R. Torre, arXiv:1512.05333 [hep-ph].
[19] E. Molinaro, F. Sannino, N. Vignaroli, arXiv:1512.05334 [hep-ph].
[20] B. Dutta, Y. Gao, T. Ghosh, I. Gogoladze, T. Li, arXiv:1512.05439 [hep-ph].
[21] S. Matsuzaki, K. Yamawaki, arXiv:1512.05564 [hep-ph].
[22] A. Kobakhidze, F. Wang, L. Wu, J.M. Yang, M. Zhang, arXiv:1512.05585 [hep-ph].
[23] R. Martinez, F. Ochoa, C.F. Sierra, arXiv:1512.05617 [hep-ph].
[24] P. Cox, A.D. Medina, T.S. Ray, A. Spray, arXiv:1512.05618 [hep-ph].
[25] D. Becirevic, E. Bertuzzo, O. Sumensari, R.Z. Funchal, arXiv:1512.05623 [hep-ph].
[26] J.M. No, V. Sanz, J. Setford, arXiv:1512.05700 [hep-ph].
[27] S.V. Demidov, D.S. Gorbunov, arXiv:1512.05723 [hep-ph].
[28] W. Chao, R. Huo, J.H. Yu, arXiv:1512.05738 [hep-ph].
[29] S. Fichet, G. von Gersdorff, C. Royon, arXiv:1512.05751 [hep-ph].
[30] L. Bian, N. Chen, D. Liu, J. Shu, arXiv:1512.05759 [hep-ph].
[31] J. Chakrabortty, A. Choudhury, P. Ghosh, S. Mondal, T. Srivastava, arXiv:1512.05767 [hep-ph].
[32] A. Ahmed, B.M. Dillon, B. Grzadkowski, J.F. Gunion, Y. Jiang, arXiv:1512.05771 [hep-ph].

[33] C. Csaki, J. Hubisz, J. Terning, arXiv:1512.05776 [hep-ph].
[34] D. Aloni, K. Blum, A. Dery, A. Efrati, Y. Nir, arXiv:1512.05778 [hep-ph].
[35] Y. Bai, J. Berger, R. Lu, arXiv:1512.05779 [hep-ph].
[36] E. Gabrielli, K. Kannike, B. Mele, M. Raidal, C. Spethmann, H. Veermäe, arXiv:1512.05961 [hep-ph].
[37] R. Benbrik, C.H. Chen, T. Nomura, arXiv:1512.06028 [hep-ph].
[38] A. Alves, A.G. Dias, K. Sinha, arXiv:1512.06091 [hep-ph].
[39] E. Megias, O. Pujolas, M. Quiros, arXiv:1512.06106 [hep-ph].
[40] L.M. Carpenter, R. Colburn, J. Goodman, arXiv:1512.06107 [hep-ph].
[41] W. Chao, arXiv:1512.06297 [hep-ph].
[42] S. Chang, arXiv:1512.06426 [hep-ph].
[43] R. Ding, L. Huang, T. Li, B. Zhu, arXiv:1512.06560 [hep-ph].
[44] X.F. Han, L. Wang, arXiv:1512.06587 [hep-ph].
[45] D. Bardhan, D. Bhatia, A. Chakraborty, U. Maitra, S. Raychaudhuri, T. Samui, arXiv:1512.06674 [hep-ph].
[46] T.F. Feng, X.Q. Li, H.B. Zhang, S.M. Zhao, arXiv:1512.06696 [hep-ph].
[47] O. Antipin, M. Mojaza, F. Sannino, arXiv:1512.06708 [hep-ph].
[48] F. Wang, L. Wu, J.M. Yang, M. Zhang, arXiv:1512.06715 [hep-ph].
[49] J. Cao, C. Han, L. Shang, W. Su, J.M. Yang, Y. Zhang, arXiv:1512.06728 [hep-ph].
[50] W. Liao, H.q. Zheng, arXiv:1512.06741 [hep-ph].
[51] J.J. Heckman, arXiv:1512.06773 [hep-ph].
[52] M. Dhuria, G. Goswami, arXiv:1512.06782 [hep-ph].
[53] X.J. Bi, Q.F. Xiang, P.F. Yin, Z.H. Yu, arXiv:1512.06787 [hep-ph].
[54] M. Bauer, M. Neubert, arXiv:1512.06828 [hep-ph].
[55] S.M. Boucenna, S. Morisi, A. Vicente, arXiv:1512.06878 [hep-ph].
[56] D. Barducci, A. Goudelis, S. Kulkarni, D. Sengupta, arXiv:1512.06842 [hep-ph].
[57] C.W. Murphy, arXiv:1512.06976 [hep-ph].
[58] A.E.C. Hernández, I. Nisandzic, arXiv:1512.07165 [hep-ph].
[59] U.K. Dey, S. Mohanty, G. Tomar, arXiv:1512.07212 [hep-ph].
[60] G.M. Pelaggi, A. Strumia, E. Vigiani, arXiv:1512.07225 [hep-ph].
[61] J. de Blas, J. Santiago, R. Vega-Morales, arXiv:1512.07229 [hep-ph].
[62] A. Belyaev, G. Cacciapaglia, H. Cai, T. Flacke, A. Parolini, H. Serôdio, arXiv:1512.07242 [hep-ph].
[63] P.S.B. Dev, D. Teresi, arXiv:1512.07243 [hep-ph].
[64] W.C. Huang, Y.L.S. Tsai, T.C. Yuan, arXiv:1512.07268 [hep-ph].
[65] K.M. Patel, P. Sharma, arXiv:1512.07468 [hep-ph].
[66] M. Badziak, arXiv:1512.07497 [hep-ph].
[67] S. Chakraborty, A. Chakraborty, S. Raychaudhuri, arXiv:1512.07527 [hep-ph].
[68] Q.H. Cao, S.L. Chen, P.H. Gu, arXiv:1512.07541 [hep-ph].
[69] W. Altmannshofer, J. Galloway, S. Gori, A.L. Kagan, A. Martin, J. Zupan, arXiv:1512.07616 [hep-ph].
[70] M. Cvetič, J. Halverson, P. Langacker, arXiv:1512.07622 [hep-ph].
[71] B.C. Allanach, P.S.B. Dev, S.A. Renner, K. Sakurai, arXiv:1512.07645 [hep-ph].
[72] H. Davoudiasl, C. Zhang, arXiv:1512.07672 [hep-ph].
[73] K. Das, S.K. Rai, arXiv:1512.07789 [hep-ph].
[74] K. Cheung, P. Ko, J.S. Lee, J. Park, P.Y. Tseng, arXiv:1512.07853 [hep-ph].
[75] J.C. Park, S.C. Park, arXiv:1512.08117 [hep-ph].
[76] A. Salvio, A. Mazumdar, arXiv:1512.08184 [hep-ph].
[77] G. Li, Y.n. Mao, Y.L. Tang, C. Zhang, Y. Zhou, S.h. Zhu, arXiv:1512.08255 [hep-ph].
[78] Y.L. Tang, S.h. Zhu, arXiv:1512.08323 [hep-ph].
[79] J. Cao, F. Wang, Y. Zhang, arXiv:1512.08392 [hep-ph].
[80] F. Wang, W. Wang, L. Wu, J.M. Yang, M. Zhang, arXiv:1512.08434 [hep-ph].
[81] C. Cai, Z.H. Yu, H.H. Zhang, arXiv:1512.08440 [hep-ph].
[82] Q.H. Cao, Y. Liu, K.P. Xie, B. Yan, D.M. Zhang, arXiv:1512.08441 [hep-ph].
[83] J.E. Kim, arXiv:1512.08467 [hep-ph].
[84] W. Chao, arXiv:1512.08484 [hep-ph].
[85] F. Goertz, J.F. Kamenik, A. Katz, M. Nardecchia, arXiv:1512.08500 [hep-ph].
[86] L.A. Anchordoqui, I. Antoniadis, H. Goldberg, X. Huang, D. Lust, T.R. Taylor, arXiv:1512.08502 [hep-ph].
[87] P.S.B. Dev, R.N. Mohapatra, Y. Zhang, arXiv:1512.08507 [hep-ph].
[88] N. Bizot, S. Davidson, M. Frigerio, J.-L. Kneur, arXiv:1512.08508 [hep-ph].
[89] C.W. Chiang, M. Ibe, T.T. Yanagida, arXiv:1512.08895 [hep-ph].
[90] S.K. Kang, J. Song, arXiv:1512.08963 [hep-ph].
[91] Y. Hamada, T. Noumi, S. Sun, G. Shiu, arXiv:1512.08984 [hep-ph].
[92] A.E.C. Hernández, arXiv:1512.09092 [hep-ph].
[93] Y. Jiang, Y.Y. Li, T. Liu, arXiv:1512.09127 [hep-ph].
[94] L. Marzola, A. Racioppi, M. Raidal, F.R. Urban, H. Veermäe, arXiv:1512.09136 [hep-ph].
[95] A. Dasgupta, M. Mitra, D. Borah, arXiv:1512.09202 [hep-ph].
[96] P. Ko, Y. Omura, C. Yu, arXiv:1601.00586 [hep-ph].
[97] W. Chao, arXiv:1601.00633 [hep-ph].
[98] A. Karozas, S.F. King, G.K. Leontaris, A.K. Meadowcroft, arXiv:1601.00640 [hep-ph].
[99] T. Modak, S. Sadhukhan, R. Srivastava, arXiv:1601.00836 [hep-ph].
[100] F.F. Deppisch, C. Hati, S. Patra, P. Pritimita, U. Sarkar, arXiv:1601.00952 [hep-ph].
[101] Q.H. Cao, Y. Liu, K.P. Xie, B. Yan, D.M. Zhang, arXiv:1512.05542 [hep-ph].
[102] P. Agrawal, J. Fan, B. Heidenreich, M. Reece, M. Strassler, arXiv:1512.05775 [hep-ph].
[103] A. Falkowski, O. Slone, T. Volansky, arXiv:1512.05777 [hep-ph].
[104] J. Gao, H. Zhang, H.X. Zhu, arXiv:1512.08478 [hep-ph].
[105] C. Csaki, J. Hubisz, S. Lombardo, J. Terning, arXiv:1601.00638 [hep-ph].
[106] A.D. Martin, W.J. Stirling, R.S. Thorne, G. Watt, Eur. Phys. J. C 63 (2009) 189, arXiv:0901.0002 [hep-ph].
[107] I.F. Ginzburg, G.L. Kotkin, S.L. Panfil, V.G. Serbo, V.I. Telnov, Nucl. Instrum. Methods, Sect. A 219 (1984) 5.
[108] I.F. Ginzburg, G.L. Kotkin, Eur. Phys. J. C 13 (2000) 295, arXiv:hep-ph/9905462.
[109] Y. Mambrini, G. Arcadi, A. Djouadi, arXiv:1512.04913 [hep-ph].
[110] H. Han, S. Wang, S. Zheng, arXiv:1512.07992 [hep-ph].
[111] K. Ghorbani, H. Ghorbani, arXiv:1601.00602 [hep-ph].
[112] G.J. Gounaris, P.I. Porfyriadis, F.M. Renard, Eur. Phys. J. C 9 (1999) 673, arXiv:hep-ph/9902230.
[113] G.J. Gounaris, J. Layssac, P.I. Porfyriadis, F.M. Renard, Eur. Phys. J. C 10 (1999) 499, arXiv:hep-ph/9904450.
[114] G.J. Gounaris, J. Layssac, P.I. Porfyriadis, F.M. Renard, Eur. Phys. J. C 13 (2000) 79, arXiv:hep-ph/9909243.
[115] J. Alwall, et al., J. High Energy Phys. 1407 (2014) 079, arXiv:1405.0301 [hep-ph].
[116] T. Behnke, et al., arXiv:1306.6329 [physics.ins-det].